TRANSPORT AND ROAD RESEARCH LABORATORY
Department of Transport

RESEARCH REPORT 67

THE PREDICTION OF SATURATION FLOWS FOR ROAD JUNCTIONS CONTROLLED BY TRAFFIC SIGNALS

by R M KIMBER (TRRL)
and M McDONALD and N B HOUNSELL (Southampton University)

The views expressed in this Report are not necessarily those of the Department of Transport

Traffic Systems Division
Traffic Engineering and Control Department
Transport and Road Research Laboratory
Crowthorne, Berkshire, RG11 6AU
1986

ISSN 0206-5247

CONTENTS

THE PREDICTION OF SATURATION FLOWS FOR ROAD JUNCTIONS CONTROLLED BY TRAFFIC SIGNALS

ABSTRACT

This report describes a comprehensive programme of measurement of saturation flow at traffic signals, and the development of prediction formulae which update those published by Webster and Cobbe in 1966, since when many factors have changed. Data were collected at 64 public road sites in UK, and the formulae based on them cover the influence on saturation flow of lane width, traffic composition, lost time, and gradient, inter alia, and deal with opposed and unopposed right-turning traffic movements. The saturation flow given for a non-nearside lane of width 3.2 m is 2080 pcu/h, some 15 per cent higher than that implied by Webster's work for his 'normal' sites.

1 INTRODUCTION

An ability to predict saturation flows is crucial to the design of road junctions controlled by traffic signals. For those existing junctions which are sufficiently loaded with traffic, the saturation flows can be measured directly using standard techniques. But at the design stage for a new junction that is not possible and it is necessary to make predictions from other, known, quantities—such as the number of lanes, the gradient of the road, and so on. To do this, generalised predictive formulae are needed.

The formulae in present use were developed by Webster and Cobbe (1966) from data now 25–30 years old. In the meantime a number of things have changed, particularly vehicle performance and road markings and layout practice. In addition, certain aspects were not treated in a very suitable way for use in modern signal optimising methods; for example, rather more structured descriptions are now needed for the complicated processes involving mixtures of straight-ahead and right-turning vehicles without a dedicated phase.

Several large scale studies have therefore been conducted recently as part of a programme to develop new formulae suitable for current conditions. A full-scale track experiment (Kimber and Semmens 1982 (a,b)) was used first, to investigate the basic relations between saturation flow and its determinants, under a wide range of conditions. Single and multilane effects were investigated for conventional and novel designs of junctions. The results for individual lanes carrying single traffic movements (eg all traffic moving straight ahead, or all turning left) were subsequently investigated in public road conditions by Martin and Voorhees Associates (Martin and Voorhees Associates 1981, Kimber, Semmens and Shewey 1982) under TRRL contract, and by Southampton University (McDonald and Hounsell 1982) under DTp contract.

The final stage in the development of predictive formulae for conventional junctions was to extend the public road studies to include multi-lane saturation flows, the effects of mixtures of turning and non-turning traffic in individual lanes, and a range of similar effects. The Transportation Research Group at Southampton University was appointed under contract to TRRL to collect and analyse saturation flow data for such cases. This Report describes the results obtained, and the development of a framework of predictive formulae from them.

2 THE DATA BASE

2.1 SELECTION OF PUBLIC ROAD SITES

Sixty-four sites were selected to provide the present data base. Table 1 gives the site locations and categories and Table 2 summarises the mean values and ranges of the more important site characteristics. As far as possible, the sites were selected for freedom from traffic disturbances arising from parked vehicles and heavy pedestrian activity. Such sites would be classified as 'poor' in the terms defined by Webster and Cobbe; the present data apply to 'good' or 'average' sites in those terms. A broad regional spread of site locations was achieved.

2.2 DATA COLLECTION METHODS

Data were collected either on site by observers using event recorders (or, occasionally, paper and pencil), or were extracted later from video recordings of the traffic at the site. The event records allowed individual vehicle departure headways to be identified.

Vehicles were classified according to the categories:

Light vehicles —3 or 4 wheeled vehicles
Medium commercial vehicles—vehicles with 2 axles but more than 4 wheels
Heavy commercial vehicles —vehicles with more than 2 axles
Buses and Coaches
Motorcycles
Bicycles

Lane-specific traffic observations in up to three adjacent lanes were recorded simultaneously. Where traffic was subject to opposing flows records were made of the discharge times of opposing vehicles classified by turning movement, and the times at

TABLE 1

Sites surveyed

Entry No.	Location	Site[1]	Direction[2]	Turning movements surveyed[3]
1	Southampton	Bursledon Rd/Kathleen Rd	W	A
2	Southampton	The Avenue/Burgess Rd	S	A
3	Bournemouth	Bournemouth Rd/Christchurch Rd	N	AL
4	Bournemouth	Waterloo Rd/Sopers Lane	N	AL
5	Southampton	Hill Lane/Archers Rd	S	AL
6	Sheffield	Upper Hanover Street/Glossop Rd	S	AL
7	Sheffield	Myrtle Rd/Bramall Lane	N	AL
8	Sheffield	Upper Hanover Street/Glossop Rd	N	AL
9	Leicester	Blackbird Rd/Anstey Lane	N	AL, A
10	Leicester	Abbey Lane/Thurcasten Rd	S	AL, A
11	Leicester	Welford Rd/Chapel Lane	S	AL, A
12	Leicester	Welford Rd/Chapel Lane	N	AL, A
13	Leicester	Welford Rd/Aylestone Road	S	A, A, A
14	Leicester	Aylestone Rd/Walnut Rd	N	A, A, A
15	Gillingham	Rainham Rd/Nelson Rd	E	AL
16	Chatham	Chatham Hill/Luton Rd	W	AL
17	London	North Circular Rd/Long Lane	E	AL
18	London	Cambridge Park/Blake Hall Rd	W	AL, A
19	London	Gt. Cambridge Road/Church Street	N	AL, A
20	London	Gt. Cambridge Road/Carterhatch Lane	S	AL, A, A
21	London	Hounslow Rd/Uxbridge Rd	S	AL
22	London	Hounslow Rd/Uxbridge Rd	N	AL
23	London	The Causeway/Great South West Rd	N	AL, A
24	London	Great West Rd/Sutton Court Rd	E	A, A, A
25	Leeds	Meadow Lane/Hunslet Rd	S	A, A
26	Leeds	York Rd/Marsh Lane	W	A, ARU
27	Leeds	Marsh Lane/York Rd	N	AL, ARU
28	Leeds	Marsh Lane/York Rd	S	A, ARU
29	Leicester	Aylestone Rd/Wigston Lane	N	AL, A
30	Leicester	Narborough Road/Braunstone Lane	S	A, A
31	Leicester	Loughborough Road/Greengate Lane	S	AL, ARO
32	Birmingham	Stratford Rd/School Road	S	AL, ARO
33	Birmingham	Hagley Rd/Rotten Park Rd	E	AL, ARO
34	Birmingham	Hagley Rd West/Bearwood Rd	W	AL, A, A
35	Birmingham	Hagley Rd West/Bearwood Rd	E	AL, A, A
36	Southampton	The Avenue/Lodge Rd	N	A, RO
37	London	Sterling Way/Upper Fore Street	W	AL, A
38	Coventry	Anstey Road/Hall Lane	N	AL, A
39	Coventry	Anstey Road/Hall Lane	S	AL, ARO
40	Leeds	Otley Road/Shaw Lane	N	AL, ARO
41	Leeds	Roundhay Road/Harehills Lane	W	A, A
42	Bradford	Queens Road/Kings Road	E	AL, ARO
43	Bradford	Queens Road/Kings Road	W	AL, ARO
44	Sheffield	Western Bank Brook/Clarkson St	W	A
45	Bradford	Queens Road/Manningham Lane	N	AL
46	Wakefield	Flanshaw Road/Dewsbury Road	S	AL, ARU
47	Bradford	Leeds Old Road/Killingham Lane	S	AL, ARO
48	Bristol	Wells Road/Airport Road	S	AL, ARU
49	Bristol	Wells Road/Airport Road	N	AL, ARU
50	Leeds	York Road/Harehills Lane	W	AL, A, A
51	London	Southend Arterial Road/Heath Road	W	AL, A, A
52	Huddersfield	Castlegate/Westgate	N	A, A
53	London	Eastern Avenue/Hainault Road	E	A, A
54	London	Great West Road/Sutton Lane	W	AL, A
55	Birmingham	Stratford Road/School Road	N	AL

TABLE 1—*continued*

Entry No.	Location	Site[1]	Direction[2]	Turning movements surveyed[3]
56	Huddersfield	Westgate/Castlegate	W	AL
57	Leeds	York Road/Harehills Lane	W	A, A, ARO
58	Leicester	London Road/Stoughton Road	S	ARO
59	London	Great West Road/Sutton Lane	W	ARO
60	Birmingham	Stratford Road/School Road	N	ARO
61	Leeds	Bridge Road/Abbey Road	E	RO
62	Leeds	Abbey Road/Bridge Road	S	RO
63	Leeds	Woodhouse Lane/Clarendon Road	S	A, ARO
64	Southampton	The Avenue/Lodge Road	N	RO

Notes 1 The first road name is the one surveyed.
2 N = northbound; E = eastbound; S = southbound; W = westbound (for ahead-only movements).
3 A = Ahead-only; AL = Ahead/left; ARU = Ahead/right unopposed;
ARO = Ahead/right opposed; RO = Right Turn Only opposed.

TABLE 2

Main site characteristics: unopposed lanes

Variable	Statistics			
	Unit	Range	Mean	Standard Deviation
Saturation Flow per Lane	pcu/h	1573 to 2293	1951	168
Initial Lost Time	s	0.16 to 2.73	1.35	0.50
End Lost Time	s	−2.34 to 3.17	0.13	1.10
Lane Width	m	2.2 to 4.4	3.25	0.39
Stop Line Width	m	3.1 to 10.2	7.44	2.16
Gradient (uphill positive, downhill negative)	per cent	−7.3 to 8.7	−0.25	2.96
Radius of turn	metres	6 to 35	16.51	5.34
Lane Number[1]	—	1 to 3		
Number of Lanes at Entry	—	1 to 3	2.25	0.68
Average Cycle Time	s	58 to 130	97.30	18.60
Average Green Time	s	19 to 81	43.90	15.50
Average Percentage of Commercial Vehicles[2]	per cent	1 to 33	7.77	6.38
Average Proportion of Turning Vehicles	—	0 to 1	0.26	0.26
Average Degree of Saturation	—	.25 to 1.0	0.67	0.34
Time of Day (a.m. peak, p.m. peak)	—	—	—	—
Webster-Cobbe Classification (poor site = 1; average site = 2; Good Site = 3	—	2, 3	—	—
Turning Movement (ahead-only, ahead/left, ahead/right)	—	—	—	—
Regional Variation (South, Leicester, London, Birmingham/ Coventry, Yorkshire)	—	—	—	—
Road Condition (dry, wet)	—	—	—	—

Notes 1 For nearside lane, L = 1, then numbered consecutively outwards.
2 Includes medium and heavy commercial vehicles and buses/coaches

which right-turners in the lane under study discharged from the intersection (as they crossed the centre line of the road). A time base of resolution 0.01 seconds was superimposed onto video records for use in subsequent analysis.

Observers also noted when the last vehicle in the queue when the signal turned green subsequently crossed the stopline. This enabled cross checks to be made using the flow in this period as an unbiassed estimator of the saturation flow.

3 RESULTS: UNOPPOSED MOVEMENTS

This section considers traffic streams which have unconditional priority in the green phase, ie those for which there was no requirement for any right-turning vehicles to give way to oncoming traffic from the opposite arm of the junction ('opposing' traffic).

3.1 CALCULATION OF THE SATURATION FLOW AND LOST TIME

The definitions used for saturation flow and lost time are well established. Figure 1 illustrates the average flow profile for the discharge of vehicles from one arm of a signal controlled intersection, during a fully saturated green period. The profile is usually represented by an 'effective green' period (BC), throughout which flow is assumed to occur at the saturation rate, and periods of 'lost time' at the beginning and end when no flow takes place. The curve in Figure 1 is then represented by a rectangle of equal area, where the height is the saturation flow and the total lost time (AB and CD) is equal to the combined green and amber periods minus the effective green time. Values of saturation flow and lost time were calculated using the standard methods of Road Note 34 (Road Research Laboratory 1963).

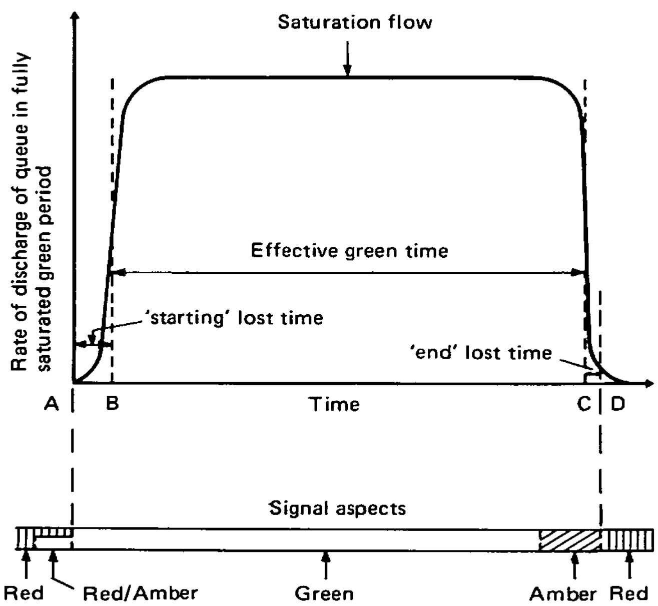

Fig. 1 Illustration of saturation flow and lost times at traffic signals

3.2 ALLOWING FOR THE EFFECTS OF TRAFFIC COMPOSITION

Saturation flows measured in vehicles per hour depend on the proportion and type of vehicles in the traffic stream. It is, therefore, usual practice to assign weighting factors (passenger car units) to the various categories of vehicle so that flows can be corrected to the common base of passenger car units per hour (pcu/h).

In principle, the effects of commercial vehicles, buses, and two-wheelers on the saturation flow may depend on the junction characteristics. For example, heavy vehicles may be more affected by gradient than cars. Such effects could be represented by pcu factors that are functions of the junction characteristics. It has been the practice in the UK, however, to use constant pcu factors, independent of the junction geometry. Possible interactions between the effects of traffic composition and junction geometry and environmental characteristics have, therefore, been investigated in the present data base, by multivariate regression analysis. No significant interaction effects were apparent, however.

In view of these results, constant pcu values are employed in the following analysis. Except for two-wheelers they were calculated by the method of headway ratios (Scraggs 1964), on a lane-specific basis. In this method the pcu value is estimated by dividing the average headway associated with a given vehicle type by that for light vehicles, corrections being necessary to cater for different numbers and combinations of vehicle types. The relationship between this and other methods is described by Kimber *et al* (1985). An average value over all lanes at each given site was then calculated. It is difficult to identify headways for two-wheelers because of their propensity to use lateral gaps between other vehicles. Prior values, taken from Kimber *et al* (1982) were therefore used. Average values over all sites for all of the vehicle categories were:

Light vehicles	1.0 (by definition)
Medium commercial vehicles	1.5
Heavy commercial vehicles	2.3
Buses and Coaches	2.0
Motorcycles	0.4
Pedal Cycles	0.2

The figures given by Webster and Cobbe are broadly similar at 2.25 for buses and coaches and 1.75 for commercial vehicles treated as a single category—nearly midway between the present values for medium and heavy commercial vehicles—and 0.33

and 0.2 for motorcycles and pedal cycles. Akcelik (1981) gives a value of 2.0 for all commercial vehicles/buses/coaches together.

3.3 SAMPLING ERROR FOR SATURATION FLOW MEASUREMENTS AT A GIVEN SITE

There are potentially three main sources of variation within the measurements: site-to-site variations, day-to-day variations at a given site, and random fluctuations between the six-second counts made at a given site on a given day. We are interested primarily in the first, but the other two limit the precision of measurement at a given site, and have therefore to be considered as well.

An analysis of variance showed that day-to-day variations did not differ significantly from within-day variations. Thus there was no evidence for, for example, differences arising out of different driver populations on different days at the same site. The precision of a saturation flow estimate at a given site could thus be estimated without separating observations made on different days: all that mattered was the total number of observations. Over all sites, the ratio of the standard deviation to the mean for the six-second counts was about 30 per cent, including all but between-site variation. The standard error of estimate at a given site was thus about $30/\sqrt{N}$ per cent, where N is the number of counts. Typically around 350 counts were used for each site, giving a precision of around $1\frac{1}{2}$ per cent or so in the saturation flow estimate for a given site.

3.4 FACTORS AFFECTING SATURATION FLOW

The factors investigated for their potential influence on the saturation flow in unopposed streams are as listed in Table 2. Appendix A summarises the notation used and the units. Factors found to have a significant influence (at the ninety-five per cent confidence level) were:

- Condition of road surface: wet/dry
- Proportion of turning traffic, f
- Radius of turn, r
- Gradient, G
- Lane position (nearside, non-nearside),
- Lane width, w_ℓ
- Number of lanes at the stop line

Intercorrelations between these factors were weak. The following sections describe the derivation of models representing their effects.

3.4.1 Road Condition: Wet/Dry

Data were collected at 17 sites in both wet and dry conditions. (The terms *wet* and *dry* refer only to the road surface: rain was too sporadic to be characterised by a separate variable.) Of the 17 possible comparisons, all had saturation flows lower under wet conditions, by an average of about 6 per cent, which was statistically significant. The saturation flows in the remainder of the report are for average road conditions, ie without the wet/dry distinction.

3.4.2 Mixed Turning Traffic: The Effects of r and f

Vehicle headways for traffic following a curved path are greater on average than those for traffic following a straight path, and the saturation flow is correspondingly less. When a stream contains a mixture of turning and non-turning vehicles, the turners impede the straight-ahead vehicles. The net saturation flow of the mixture then depends on the path radius, r (Appendix A gives the units of all quantities), and the proportion of turners, f. Previous work (Webster and Cobbe (1966); Kimber *et al* (1982); McDonald and Hounsell (1984)) has shown that for f = 1 (ie all turning traffic), the equation

$$S(r) = S_a/(1 + 1.5/r) \qquad \ldots(1)$$

provides a good prediction of the saturation flow, S(r), for turning traffic where S_a is the saturation flow for straight-ahead traffic. In the present work the objective is to formulate an expression describing the relation between the saturation flow and both r and f: S = S(r,f). Equation (1) is taken as a required limit for such an expression when $f \rightarrow 1$.

For mixtures in left-turn lanes, Webster and Cobbe recommended that each extra left-turner beyond a nominal 10 per cent mix (the effects of which were already present in their data base) be weighted by 1.25 to represent its effect on the saturation flow. This implied a relationship of the type

$$S(f) = \frac{S_a}{1 + (T-1)f} \qquad \ldots(2)$$

where T(= 1.25 in this case) is known as a *through car unit* (tcu) (eg see Heydecker (1982)).

However, equation (2) takes no account of radius of turn, so that if $f \rightarrow 1$, $S(f) \rightarrow S_a/1.25$, contrasted with the unmixed lane case of $S(r) = S_a/(1 + 1.5/r)$. The simplest approach in formulating a model containing both f and r is to assume that the mean inter-vehicle headway in the mixed traffic is just the weighted average of the mean headways for straight-ahead vehicles and for turning vehicles constrained by radius according to equation (1). Thus:

$$\frac{1}{S(f,r)} = \frac{1-f}{S_a} + \frac{f}{S(r)}$$

and $S(f,r) = S_a/(1 + 1.5f/r)$.

This is equivalent to putting $T = 1 + 1.5/r$ in equation (2). In fact this proved the best model of those tried. S_a was determined for lanes dedicated to left and ahead mixtures, $S_{a\ell}$, and right and ahead mixtures, S_{ar}, by averaging the saturation flows for the relevant 'mixed' lanes for those signal phases which contained no turning traffic, at sites with gradient less than 2 per cent. The result was:

$S_{a\ell} = 1940$ (21) pcu/h

$S_{ar} = 2080$ (19) pcu/h

(figures in brackets are standard errors). The difference between $S_{a\ell}$ and S_{ar} is equivalent to the difference between nearside and non-nearside lanes noted by Kimber *et al* (1982). The model therefore becomes

$$S(r,f) = \frac{2080 - 140\delta_n}{1 + 1.5f/r} \qquad \ldots (3)$$

where $\delta_n = 1$ for a nearside lane and zero otherwise. Figure 2 illustrates the predictions: although the degree of residual scatter between observed and predicted values was quite large, there was no apparent bias. Arbitrary adjustment of S_a and the coefficient of f/r did not yield any significant improvements. The effect of lane width on saturation flow (see Section 3.4.4 below) was ignored here since (a) it was small, and (b) the correlation between lane width and r was negligible in the data base.

The average curve radius for the left turn lanes was 12 m and the corresponding value of $T = 1.125$ was rather less than Webster and Cobbe's value of 1.25.

The results above for left-turning movements apply to layouts where the left turn occurs at the stop line. At some sites, however, a left turn diverging lane is provided which may or may not be under signal control. This facility is particularly useful where the proportion of left-turning vehicles is high, and in one example studied a maximum increase in saturation flow of some 30 per cent was achieved by the presence of a 30 m diverging lane in addition to the 'primary' lane carrying straight-ahead traffic. This increase was mainly due to straight-ahead vehicles closing up the gaps left when preceding left-turners diverged. The benefit would presumably be related to the length of the diverging lane. Right-turning diverging lanes are also provided at many multilane sites.

3.4.3 Gradient and Lane Position

Twenty-eight lanes had gradients of magnitude greater than 2 per cent. Assigning downhill approaches a negative gradient and uphill ones a positive gradient, the overall range was from −7.3 per cent to +8.7 per cent. The gradients were measured over a distance of 60 m upstream from the stop line, but generally persisted through the intersection and onto the exit road.
The present objective is to determine the dependence of saturation flow on gradient and lane position. The saturation flows were first corrected for the effects of turning traffic using the relation

$$S' = S(1 + 1.5f/r),$$

where S is the measured saturation flow, f and r are defined as before for lanes containing turning traffic, and S' is the corrected saturation flow equivalent to that which would be measured in an ahead-only lane. The data base was not sufficiently extensive to allow interaction effects to be investigated so the effect of turning traffic was assumed to be independent of gradient. Lane width was not significantly correlated with gradient.

Figure 3 illustrates the results. Several features are apparent:

(i) saturation flow decreases as uphill gradient increases;

(ii) there is no visible relationship between saturation flow and downhill gradient;

(iii) saturation flows are usually higher in offside lanes than in nearside lanes.

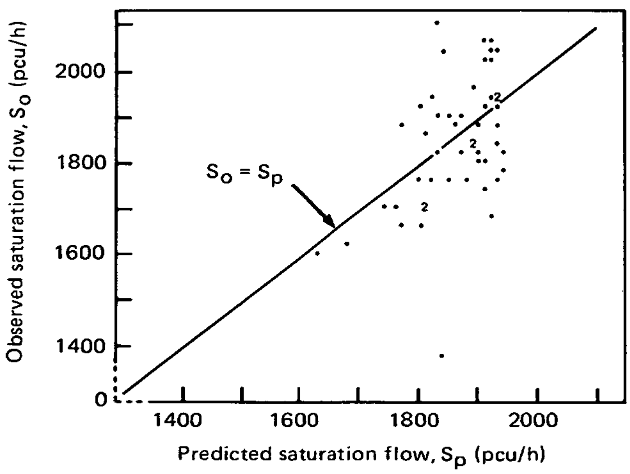

Fig. 2 Saturation flows as observed and as predicted by equation 3, for lanes containing unopposed mixed turning movement traffic. Numbers indicate multiple points

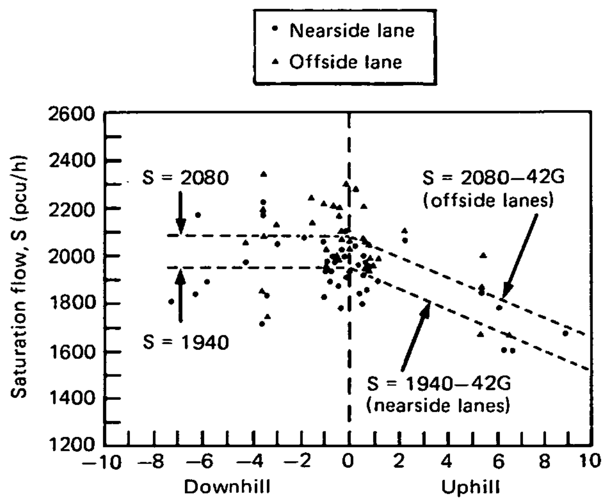

Fig. 3 Relationship between saturation flow and gradient

Each of these inferences was statistically significant. The division of non-nearside lanes into offside and non-offside (ie middle) lanes did not reveal any significant correlations with the saturation flow. Regression analysis was used to develop models relating mean saturation flow to gradient. The best were:

uphill, nearside lanes:

$$S = \underset{(38)}{1942} - \underset{(8)}{36G} \qquad \ldots(4)$$

uphill, non-nearside lanes:

$$S = \underset{(45)}{2087} - \underset{(12)}{51G} \qquad \ldots(5)$$

As before, the figures in brackets are the standard errors. The gradient coefficients were not significantly different, but the constant terms were. Moreover, the constant terms did not differ individually from the corresponding saturation flows S_{a_ℓ} and S_{ar} in the previous section. The data base for equations (4) and (5) included all individual lane observations. It seems reasonable to conclude that the saturation flows in nearside lanes are in general significantly less than for other lanes, in agreement with Kimber *et al* (1982). In view of the close similarity of the numbers, it is convenient to retain in the model the round numbers of S_{a_ℓ} and S_{ar}. Since the gradient coefficients did not differ significantly the data were pooled and a combined coefficient calculated. This was done by calculating

$$S'' = S' + 140\delta_n$$

and regressing S″ on G for uphill sites. Here n denotes lane position (nearside/non-nearside), $\delta_n = 1$ for a nearside lane and zero otherwise and its coefficient represents the difference (2080 – 1940 pcu/h) between non-nearside and nearside lanes. The resulting gradient coefficient was 42 pcu/h with standard error 7 pcu/h. So the overall result becomes:

$$S'(n,G) = 2080 - 140\delta_n - 42G$$

Downhill sites, for which gradient had no effect, can be included by introducing a dummy variable δ_G equal to one for uphill sites and zero otherwise, to give:

$$S'(n,G) = 2080 - 140\delta_n - 42\delta_G G \qquad \ldots(6)$$

Incorporating the results of the previous section, the combined model for saturation flow, now in terms of r, f, n and G is therefore:

$$S(r,f,n,G) = (2080 - 140\delta_n - 42\delta_G G)/(1 + 1.5\ f/r) \ldots(7)$$

A 1 per cent increase in uphill gradient therefore causes a decrease in S of about 2 per cent. This contrasts with Webster and Cobbe's figure of 3 per cent. More importantly, for downhill gradients there is no effect, whereas Webster and Cobbe had a 3 per cent increase per 1 per cent increase in downhill gradient.

3.4.4 Lane Width

To investigate the effect of lane width all individual lane saturation flows were first corrected for the effects of turning traffic, gradient and lane position by calculating:

$$S''' = S(1 + 1.5\ f/r) + 140\delta_n + 42\delta_G G \qquad \ldots(8)$$

where S is the measured saturation flow and S‴ the corrected flow. S‴ was regressed on lane width, w_ℓ (expressed in terms of differences with respect to the mean lane width $\overline{w}_\ell$ over all sites, ie by regressing S‴ on $(w_\ell - \overline{w}_\ell)$, $(\overline{w}_\ell = 3.25\text{ m})$) using a linear model. The resulting coefficient for lane width was about 100 pcu/h per metre with standard error 50 pcu/h per metre; but the effect was significant only at the 10 per cent level. Regression using subsets of the data consisting of nearside lanes only or non-nearside lanes only did not produce significantly different values for the coefficient.

Lane width effects have been reported by a number of authors (see Kimber and Semmens (1982a) for a summary). They range from zero (Martin and Voorhees Associates (1981), public road data) to about 295 pcu/hm (Kimber and Semmens, test track data), compared with the present value of 100 pcu/hm. Although the present result is significant only at the 10 per cent level, it seems reasonable to retain it since there seems to be some agreement about the general trend.

3.4.5 Saturation Flow Prediction for the Single Unopposed Lane Case

The results of Sections 3.4.2–3.4.4 can be combined into a single predictor equation for the saturation flow S of a single lane:

$$S(r,f,n,G,w_\ell) = (2080 - 140\delta_n - 42\delta_G G + 100(w_\ell - 3.25))/(1 + 1.5\ f/r) \qquad \ldots(9)$$

Because of the low correlations between the 'independent' variables in this equation, this result was relatively insensitive to joint reoptimisation of the coefficients by multivariate regression.

Figure (4) shows the relationship between observed (uncorrected) and predicted values according to equation (9). The squared correlation coefficient overall was 0.52 and the rms residual,

$$\left[\sum_{k=1}^{N} (S_o - S_p)^2/(N-1)\right]^{\frac{1}{2}},$$

was 117 pcu/h, where S_o and S_p are the observed and predicted saturation flows and N is the number of measurements.

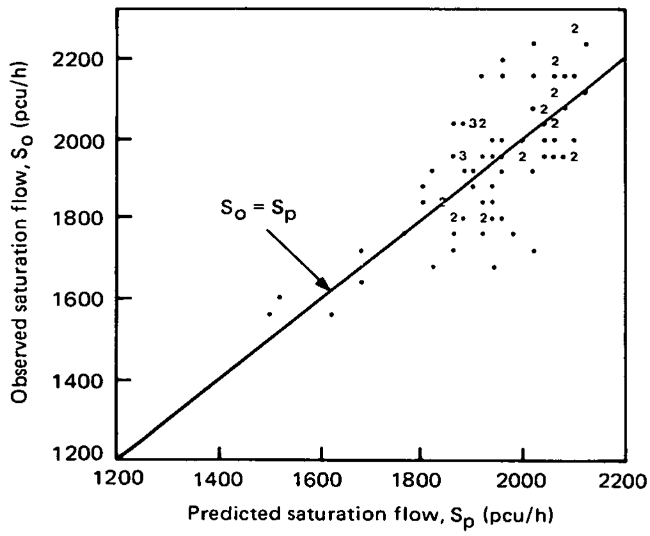

Fig. 4 Observed (S_o) versus predicted (S_p) saturation flows in lanes of unopposed mixed turning traffic Numbers indicate multiple points

3.4.6 Multilane Entries

When Webster and Cobbe's work was published it was not the general practice to mark individual lanes in the approach to the stop-line. In those circumstances the number of lanes formed by waiting vehicles within a given overall width W is variable, even in saturated conditions. Webster and Cobbe used a linear predictive relationship, $S = 527\ W$ pcu/h, for widths greater than about 5 m (ie equivalent to a wide single lane), and this presumably reflected the progressive effects of space utilisation with increasing width. For example, with $W \simeq 9$ m sometimes two queues would form, and sometimes three; as W increased so the proportion of time for which there were three queues would increase progressively.

No equivalent effect was apparent when the present observations were made, motorists keeping systematically to lanes, with the exception of some two-wheelers, who contribute relatively little to the net saturation flow in pcu/h. Figure 5 illustrates the width-dependence of the saturation flows. Superimposed are the predictions of three models:

(i) $S = \sum_i S_i$, where S_i is the saturation flow predicted for each lane by equation (9) above;

(ii) Webster and Cobbe's (1966) model;

(iii) $S = kW$, a simple linear model.

Of these, the first is significantly better than the other two. Importantly, the linear dependence of S on width for a given number of lanes is much too large for the simple linear model, (iii), which would imply a within-lane width dependence of about 600 pcu/h per metre compared with the value of 100 (SE 50) pcu/h per metre obtained in Section 3.4.4. (It is difficult to find public road sites which allow the dependence on lane width to be tested exactly for multilane stop lines with extremely narrow lanes, however; and for

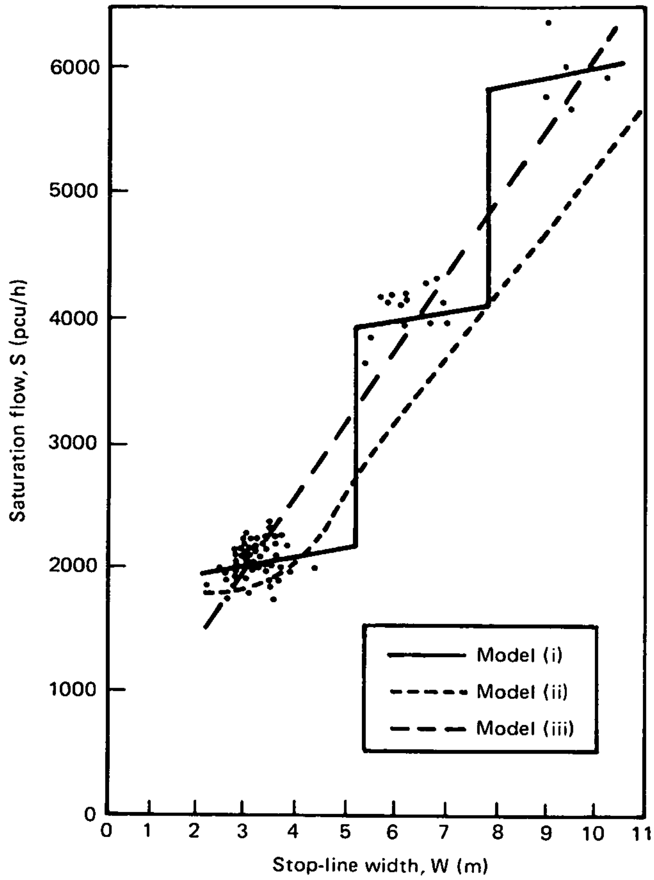

Fig. 5 Relationship between saturation flow and full stop-line width (see text, Section 3.4.6 for definitions of models) Vertical lines on the model (i) plot indicate approximate limits on the range of width for which a given number of lanes was marked (~5m for 1–2 lanes, 8m for 2–3 lanes)

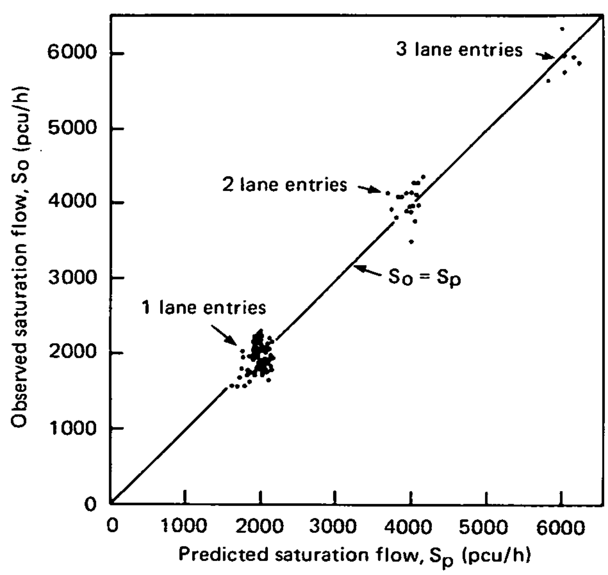

Fig. 6 Observed against predicted saturation flows for multi-lane entries containing unopposed traffic according to Model (i)
(see Section 3.4.6)

lanes narrower than the lower limit of the range given in Table 2, it would be wise to expect a very rapid deterioration in saturation flow with decreasing width.)

The general underprediction of model (ii) would be lessened if allowance were made for Webster and Cobbe's 'site quality' factor, which allowed a 20 per cent increase in saturation flow for 'good' sites. About 70 per cent of the present sites would have been classified as good in those terms. However, no significant residual correlation was apparent between the site quality factors (which were always 'good' or 'average', never 'poor') and the saturation flows. So there is no evidence within the present data to suggest that the correction should, in fact, be applied. Martin and Voorhees found a similar result. There seems therefore to have been a substantive percentage increase in saturation flows since Webster and Cobbe's data were obtained.

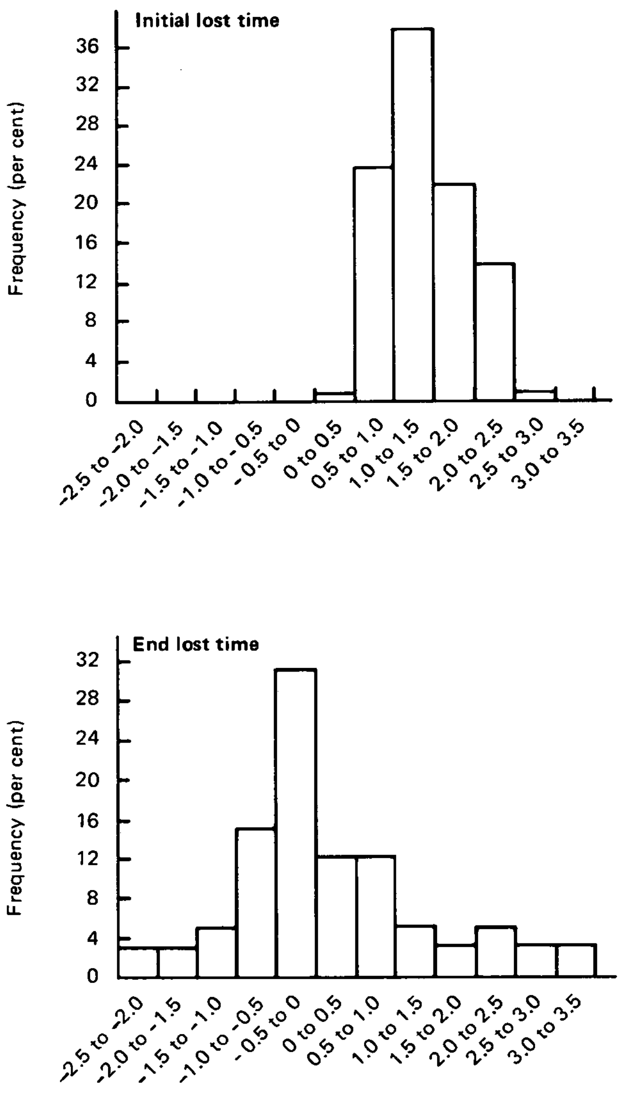

Fig. 7 Distribution of initial and end lost times (s)

In view of these results, the best approach for prediction is therefore simply to use equation (9) for the individual lanes and then to sum the resulting saturation flows over the whole entry. Figure (6) shows the relation between observed (uncorrected) and predicted data using this model.

3.5 LOST TIMES

As in previous studies, site-specific lost times showed no correlation with any site descriptors. Figure 7 shows the distribution between sites. The average starting lost time was 1.35 s and the standard deviation over the site-mean values was 0.5 s; corresponding figures for the end lost time were 0.13 s and 1.1 s respectively.

4 RESULTS: OPPOSED MOVEMENTS

This section describes the analysis of saturation flow data for lanes containing mixtures of straight-ahead and opposed right-turning traffic. Data are characteristically more variable in this case, where drivers wishing to turn right have to decide whether or not they can safely cross during gaps in the opposing flow. Moreover, it is difficult to obtain data spanning a wide range of the relevant parameters. The analysis was therefore done in two stages. In the first, a vehicle-vehicle simulation model was set up using an assumed set of rules for the vehicle interactions. Data were then simulated by running the model for wide ranges of the relevant input parameters and a predictive model derived to represent the results. In the second stage this model was tested and recalibrated against the public road data.

4.1 DEFINITION OF SATURATION FLOW

The assumption of constant saturation flow preceded and followed by periods of lost time as in Figure 1 is clearly not applicable when there is an opposing flow and right-turners have to wait for gaps in this flow before moving off. The saturation flow was therefore taken as the average rate of discharge of straight-ahead plus right-turning vehicles during the period of saturation (ie steady queueing). There is no lost time in this description. The period of discharge was taken to include the initial time during which the opposing flow itself was saturated, since for lanes containing mixed ahead and right-turning traffic there can be a significant initial flow if a sequence of ahead-only vehicles occurs at the beginning of the phase. To exclude this time would therefore be misleading in this case, although it can be done for dedicated right-turn lanes where no departures occur during the initial period of saturation of the opposing flow (see Kimber and Semmens (1982a)).

4.2 SIMULATION

The development of the simulation model for the case where opposed right-turners are present in the offside lane is described in Appendix B. The saturation flows generated by the model were found to depend mainly on the following factors:

- the intensity of traffic (the demand flow divided by the 'capacity' per cycle) on the *opposing* arm, X_o
- the proportion of right-turning traffic, f
- the number of storage spaces available within the intersection which right-turners can use without blocking straight-ahead traffic, N_s
- the number of signal cycles per hour 3600/c (where c is the cycle time in seconds).

Two components of flow were identified: S_g, corresponding to the departures of vehicles during the effective green period; and S_c, corresponding to departures immediately after the end of effective green (the 'clearance' component).

Appendix B also describes the development of a predictive model which enables the saturation flow to be estimated from the parameters X_o, f, N_s, λ, and c:

$$S = S_g + S_c \quad \text{pcu per hour of effective green} \qquad \ldots(10)$$

where $S_g = A/(1 + (T-1)f)$

$S_c = P(N_s + 1)(fX_o)^{0.2}.3600/\lambda c$

and T is, as before, the tcu value of a right-turning vehicle, but it now depends on X_o and N_s as well as f and r (the effects of r were not explicitly represented in the simulation, but are assumed to be as before):

$T = 1 + 1.5/r + t_1/t_2$

where $t_1 = aX_o^n/(1-(fX_o)^m)$

$t_2 = 1 + b(1-f)N_s$

$X_o = q_o c/S_o g$.

q_o, S_o are the arrival rate and saturation flow in the *opposing* stream and g the effective green time for it. a, b, n, and m are fitting constants, and A (pcu/h) represents the saturation flow of straight-ahead traffic. P is a conversion factor from veh/h to pcu/h: $P = 1 + \sum_i (\alpha_i - 1)p_i$ where p_i is the proportion of vehicles of type i and α_i the corresponding pcu value. Values for the fitting constants were determined by hill-climbing techniques designed to minimise the sum of squares of residual differences between the simulated data and the values predicted from equation (10). The values obtained were: a = 10, b = 0.6, n = m = 2. Figure 8 shows a plot of simulated saturation flows against those predicted by equation (10), using these values.

It should be noted that S_c is defined above so as to give the effective contribution of the clearance process to the saturation flow per hour of continuous green. That makes it homogeneous with S_g. In reality the clearance occurs discontinuously between phases.

The next stage in developing the model is to recalibrate it against public road data.

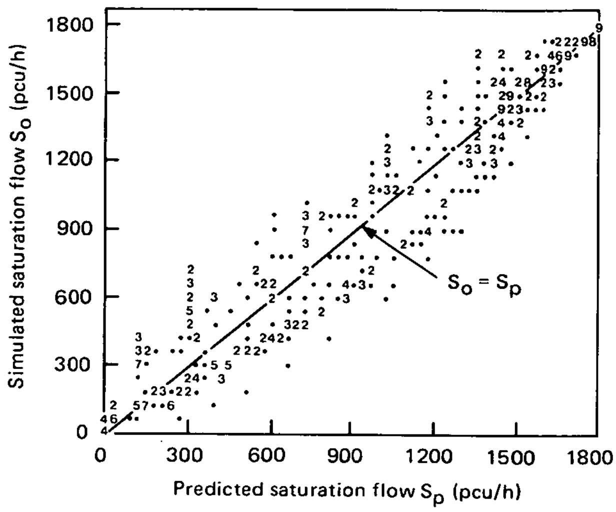

Fig. 8 Simulated versus predicted saturation flows for lanes containing opposed mixed turning movement traffic from simulated data. Predictions are by equation (10), numbers indicate multiple points

4.3 RESULTS OF PUBLIC ROAD MEASUREMENTS

Data were collected at eleven sites. Table 3 lists the main site characteristics. The analyses followed the same lines as with the simulated data (Appendix B). The saturation flows were correlated with the opposing flow and with the proportion of right-turners. The opposing flow was subdivided in the measurements into its three components: straight-ahead, left-turning, and right-turning. Right turns were non-hooking in all cases. In accordance with previous work they were therefore excluded from q_o, the total flow on the opposite arm; left-turners were included. There was no significant correlation with N_s, although it is likely that this was due mainly to the intrinsically high random variability of the data.

The simulation model was recalibrated against the public road data by adjusting the fitting constants until a new minimum was found in the sum of squared residuals. This resulted only in a change of a, from a = 10 to a = 12. The saturation flow, A, for straight-ahead vehicles was determined by averaging over all phases free of right-turners. The average over all sites was 1850 pcu/h. The fact that this is some 230 pcu/h less than the value for streams not containing opposed right-turners presumably reflects the greater uncertainties for straight-ahead drivers when opposed right-turners may be present.

TABLE 3

Main site characteristics: opposed lanes

Variable	Unit	Statistics		
		Range	Mean	Standard Deviation
Saturation Flow	pcu/h	88 to 2418	966	626
Opposing Flow	vehs/h	136 to 4205	1533	1076
Proportion of right turners		0 to 1	0.54	0.40
Lane Width	m	2.6 to 3.8	3.20	0.50
Gradient (uphill +ive downhill −ive)	per cent	−0.7 to 2.9	0.20	1.60
Radius of turn	m	5 to 22	12	7.40
Average cycle time	s	68 to 119	95	21
Average green time	s	26 to 60	44	14
Storage space		0 to 5		
Number of opposing lanes		2, 3		

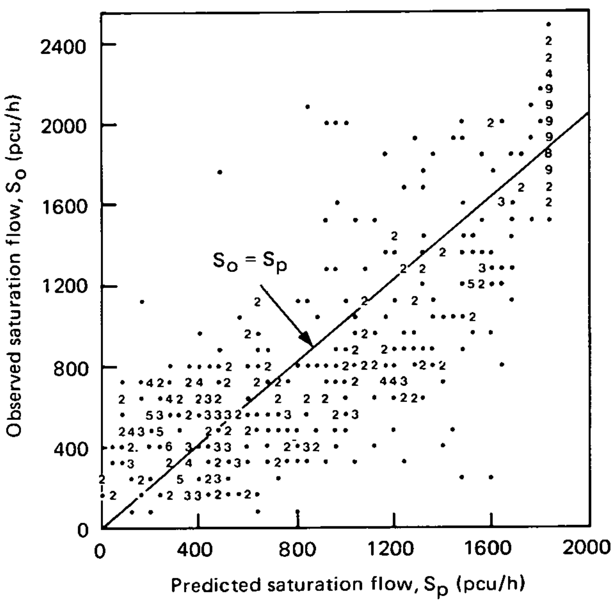

Fig. 9 Observed against predicted saturation flows for lanes containing opposed mixed turning movement traffic from phase-by-phase public road data. Predictions are by equation (10), recalibrated as in Section 4.3. Numbers indicate multiple points

Figure 9 shows a plot of observed saturation flow data (phase-specific) against the values predicted by equation (10). The increase in scatter compared to Figure 8 is largely attributable to the fact that the comparison is phase by phase rather than for very long term averages. Overall there was no apparent bias in the model. The rms residual for site mean predictions was 180 pcu/h.

(It is worth remarking at this point that, for new designs, the proportion of right-turners, f, will only normally be known for the entry as a whole. The value of f in the offside lane alone will depend on the number of straight-ahead drivers who decide to use this lane. This decision will normally be based on the driver's estimation as to which lane will result in him suffering least delay. Thus, the value f can be estimated by calculating the delay to straight-ahead traffic in the offside and adjacent lanes separately for various levels of f (see Section 4.5) and using that value which results in equal delays to straight-ahead traffic in each lane.)

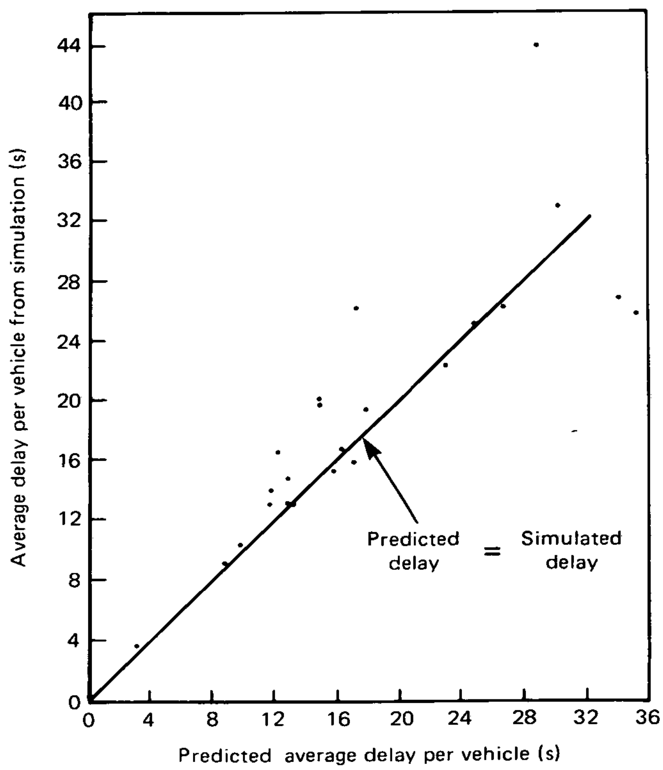

Fig. 10 Comparison of average delays per vehicle obtained from simulation and predicted from equations (10) and (12)

4.4 COMBINING THE EFFECTS

In the sections treating opposed flows, A has so far been regarded as a constant. The data do not allow dependence on other variables to be inferred. However, it seems reasonable to suppose that were they not masked by the extra variability associated with the opposed right-turn movements, the effects of relevant variables which influenced other movements (section 3) would be apparent. Thus uphill gradients would influence the saturation flow of mixtures containing opposed right-turners, as would differences in lane width. So it seems reasonable to write $A = 1850 - 42\delta_G G + 100(w_t - \overline{w}_t) = (S_o - 230)$ pcu/h in place of $A = 1850$ pcu/h, giving

$$\left.\begin{aligned} & S = S_g + S_c \\ \text{where} \quad & S_g = (S_o - 230)/(1 + (T-1)f) \\ & S_c = P(1 + N_s)(fX_o)^{0.2}\, 3600/\lambda c \\ \text{and} \quad & T = 1 + 1.5/r + t_1/t_2 \\ & t_1 = 12X_o^2/(1 + 0.6(1-f)N_s) \\ & t_2 = 1 - (fX_o)^2 \end{aligned}\right\} \quad \ldots(11)$$

4.5 VEHICLE DELAYS

The formula developed in Sections 3 and 4 above can be used to provide saturation flow estimates for input to delay models in the usual way. Delays to vehicles in lanes containing mixtures of ahead and *opposed* right-turning traffic have not been explicitly dealt with previously (eg by Webster and Cobbe (1966)) and it is necessary therefore to see how well the present formulae for saturation flows perform as a basis for delay estimation models.

Estimates of vehicular delay were therefore obtained from the simulation model of Appendix B. A predictive model for these delays was formulated from

(a) equation (10), which provided saturation flow estimates

and (b) Webster's formula, which used the saturation flow estimates and predicted the delays:

$$d = \frac{c(1-\lambda)^2}{2(1-\lambda x)} + \frac{x^2}{2q(1-x)} - 0.65\left(\frac{c}{q^2}\right)^{\frac{1}{3}} x^{(2+5\lambda)} \quad \ldots(12)$$

The results are shown in Figure 10. The delay values can be seen to be quite close in most cases, the biggest differences occurring at high values of delay which corresponded to high intensities (X_o>0.8), at which the sampling variability becomes considerable for the stochastic processes represented in the simulation (and present in real life). The estimated standard error of the population mean can be reduced by employing very long simulation periods (those used here were several hours), but the situation is then artificial since explicit account should really be taken of the dependence of the mean demand flow on time. Webster's formula is for the steady state, of course, (and so were the simulation runs) and when $X_o \geqslant 0.8$ it should really be replaced by time-dependent formulae (see Kimber and Hollis, 1979) which take Webster's formula as the steady-state limit. However, the present comparisons show that delay prediction using the above model ((a) and (b)) is satisfactory in steady-state conditions. Other published (steady-state) delay formulae were also assessed, replacing (b), but provided no improvement in the quality of agreement between simulated and predicted delays.

5 SUMMARY

A study has been made of the factors affecting saturation flows at traffic signals where there are mixtures of turning movements. Data were collected at a total of 64 public road sites. The study brings together the results of a programme of work over the past several years on saturation flow prediction. The main results are summarised below.

1. The saturation flow for a non-nearside lane of 'average' width, 3.2 m, is now around 2080 pcu/h, some 15 per cent or so higher than the equivalent implied by Webster's 1966 value of around 1800 pcu/h. For nearside lanes the present figure is about 1940 pcu/h, an increase of some 8 per cent over the Webster figure.
2. The effects of *traffic composition* can be represented by passenger car equivalent units (pcus). The following values were derived: medium commercial vehicle: 1.5 pcu; heavy commercial vehicle 2.3 pcu; bus or coach 2.0 pcu. Values for motorcycles and pedal cycles were taken from previous work as 0.4 and 0.2 pcus respectively. Cars are by definition 1.0 pcu.
3. *Lost times* were uncorrelated with site factors. The starting lost time had a mean value over all sites of 1.35 s and a standard deviation across sites of 0.5 s. Corresponding values for the end lost time were respectively 0.13 s and 1.1 s.
4. For individual lanes containing *straight-ahead* traffic, *saturation flows*:
   - decreased with uphill gradient by two per cent per one per cent of gradient, but were unaffected by downhill gradient;
   - increased with lane width, by 100 pcu/h per metre of width;
   - were lower by six per cent in wet road conditions than in the dry;
   - were lower by about 140 pcu/h in nearside lanes than in other lanes.
5. For individual lanes containing *unopposed turning traffic, saturation flows* decreased for higher proportions of turning traffic and lower radii of turn.

6. The contributions from individual lanes to the *saturation flow at multilane stoplines* where all lanes were saturated could be treated independently. The total saturation flow could be predicted as the sum of the individual lane predictions.
7. A simulation model was developed to represent the vehicle departure process from lanes containing *mixtures of straight-ahead traffic and opposed right-turning traffic*. The main factors determining the saturation flow were:
   - the traffic intensity on the opposing arm
   - the number of storage spaces available within the intersection which right-turners can use without blocking straight-ahead traffic
   - the number of signal cycles per hour.

   Predictive equations developed for the saturation flows generated by the simulation were recalibrated against data collected at the public road sites.
8. The final predictive model for the saturation flow (pcu/h) was as follows. Symbols are all as defined in Section 8.

   (a) *Unopposed streams in individual lanes*

   $S_1 = (S_0 - 140\delta_n)/(1 + 1.5\ f/r)$

   where $S_0 = 2080 - 42\delta_G G + 100(w_\ell - 3.25)$

   (b) *Streams containing opposed right-turning traffic in individual lanes*

   $S_2 = S_g + S_c$

   where: $S_g = (S_0 - 230)/(1 + (T-1)f)$

   and $T = 1 + 1.5/r + t_1/t_2$

   $t_1 = 12X_o^2/(1 + 0.6(1-f)N_s)$

   $t_2 = 1 - (fX_o)^2$

   and $S_c = P(1 + N_s)(fX_o)^{0.2}\,3600/\lambda c$

   $X_o = q_o/\lambda n_\ell s_o$

   (c) *Multilane stoplines*

   $S_3 = \sum_{\text{all lanes, i}} S_i$

   where S_i is the saturation flow for the ith lane predicted by (a) or (b) above as appropriate.

6 ACKNOWLEDGEMENTS

The work described in this report was carried out in the Traffic Systems Division (Division Head: Mr M Grimmer) of the Traffic Engineering and Control Department of TRRL.

7 REFERENCES

AKCELIK, R (1981). Traffic Signals: Capacity and Timing Analysis. *Research Report No. ARR 123.* Australian Road Research Board, Vermont.

HEYDECKER, B G (1982). Vehicles, PCU's and TCU's in Traffic Signal Calculations. *Traffic Engineering and Control, 24* (3), pp 111-114.

KIMBER, R M and HOLLIS, E M (1979). Traffic Queues and Delays at Road Junctions. *TRRL Laboratory Report* 909. Transport and Road Research Laboratory, Crowthorne.

KIMBER, R M, McDONALD, M and HOUNSELL, N B (1985). Passenger Car Units in Saturation Flows: Concept, Definition, Derivation. *Transportation Research 19B* (1), pp 39-61.

KIMBER, R M and SEMMENS, M C (1982a). An Experiment to Investigate Saturation Flows at Traffic Signal Junctions. *Traffic Engineering and Control, 23* (3), pp 110-117.

KIMBER, R M and SEMMENS, M C (1982b). Traffic Signal Junctions: A Track Appraisal of Conventional and Novel Designs. *TRRL Laboratory Report* 1063. Transport and Road Research Laboratory, Crowthorne.

KIMBER, R M, SEMMENS, M C and SHEWEY, P J H (1982). Saturation Flows at Traffic Signal Junctions: Studies on Test Track and Public Roads. *Institute of Electrical Engineers Conference on Road Traffic Signalling* (Conference publication No 207)

MARTIN AND VOORHEES ASSOCIATES (1981). Saturation Flows and Lost Times at Traffic Signal Junctions. *TRRL Working Paper TSN* 77. Transport and Road Research Laboratory, Crowthorne. (Unpublished—available on personal request only).

McDONALD, M and HOUNSELL, N B (1982). Traffic Parameters at Traffic Signals. *Technical Report by the Transportation Research Group.* Department of Civil Engineering, University of Southampton.

McDONALD, M and HOUNSELL, N B (1984). Hybrid Effects Influencing Saturation Flows at Traffic Signals. Transportation Research Group, Department of Civil Engineering, University of Southampton.

ROAD RESEARCH LABORATORY (1963.) A Method of Measuring Saturation Flow at Traffic Signals. *Road Note 34.* HMSO, London.

SCRAGGS, D A (1964). The Passenger Car Equivalent of a Heavy Vehicle in Single Lane Flow at Traffic Signals. *Road Research Laboratory Report LN/573/DAS*. Transport and Road Research Laboratory, Crowthorne.

WEBSTER, F V and COBBE, B M (1966). Traffic Signals. *Road Research Technical Paper No.* 56. HMSO, London.

8 APPENDIX A

SUMMARY OF NOTATION

The main symbols used in the text are defined below.

c Cycle time (secs)

d Average delay per vehicle (s)

δ_G Gradient dummy variable (=0 for downhill entries, and 1 for uphill entries)

δ_n Nearside lane dummy variable (=0 for non-nearside lanes, and 1 for nearside lane or single lane entries)

f Proportion of turning vehicles in a lane

g Effective green time (s)

G Gradient (per cent)

λ Proportion of the cycle which is effectively green for the phase under consideration (ie $\lambda = g/c$)

n Lane position at entry

n_ℓ Number of lanes on opposing entry

N_s Number of storage spaces available inside the intersection which right-turners can use without blocking following straight-ahead vehicles

P $1 + \sum_i (\alpha_i - 1) p_i$ where

α_i = pcu value of vehicle type i
p_i = proportion of vehicles of type i in stream

q Flow: average number of vehicles passing a given point on the road in the same direction per unit of time (vehicles per second for delay calculations)

q_o Flow on opposite arm (vehicles per hour of green time—excludes non-hooking right-turners)

r Radius of curvature of vehicle paths (m)

S Saturation flow (pcu/h)

S_a Saturation flow for ahead-only traffic in lanes of unopposed mixed turning traffic (pcu/h)

A Saturation flow for ahead-only traffic in lanes of opposed mixed turning traffic (pcu/h)

S_g Saturation flow in lanes of opposed mixed turning traffic during the effective green period (pcu/h)

S_c Saturation flow in lanes of opposed mixed turning traffic after the effective green period (veh/h or pcu/h see text)

s_o Saturation flow per lane for opposite entry (pcu/h)

T TCU (through car unit) factor of a turning vehicle in a lane of mixed turning traffic. Each turning vehicle is equivalent to 'T' straight-ahead vehicles

w_ℓ Lane width at entry (m)

$\overline{w}_\ell$ Average lane width over sites (3.25 m)

W Stop-line width (m)

x Degree of saturation in lane: the ratio of the flow to the saturation flow (ie $x = q/\lambda S$)

X_o Degree of saturation on opposing arm: the ratio of the flow on the opposing arm to the saturation flow on that arm (ie $X_o = q_o/\lambda n_\ell s_o = q_o c/g S_o$)

9 APPENDIX B

A SIMULATION-BASED MODEL OF THE OPPOSED RIGHT-TURN CASE

B.1 THE SIMULATION MODEL

A computer simulation model was set up in which hypothetical vehicles were generated upstream of the junction, moved into a queue at the stopline and were released into the junction during green periods. There they either proceeded straight ahead, or attempted to turn right. When the number of waiting right-turners exceeded a given value, the progress of straight-ahead vehicles was interrupted. Right-turners waited for suitable gaps in the opposing flow. Queueing was *first come first served* (FIFO). Table 4 summarises the parameters of the model. The main inputs included:

- the vehicle arrival and departure patterns;
- the gap acceptance characteristics for right-turning vehicles;
- the available 'storage' space N_s for waiting right-turners—when this was exceeded, straight-ahead traffic was interrupted;
- the proportion of right-turners in the lane, f;
- the signal timings.

Output consisted essentially of the mean saturation flow and vehicular delay for the lane, evaluated over many cycles of the signal.

The model was initially set up with f = 1, and the saturation flows compared with those of Kimber and Semmens (1982a) obtained under closely controlled test track conditions. The parameter values given in Table 4 resulted in the saturation flow characteristics shown in Figure B1. The saturation flows were somewhat higher than those given by Webster and Cobbe (1966), mainly because the assumed minimum headways for the opposing streams were lower (2s and zero here, for one and two-lane opposing flow respectively, compared with 3s and 1s in Webster and Cobbe (1966)). They were broadly similar to those of the test track data, however, except that the assumed gap-acceptance model for the right-turners gave a degree of non-linearity not apparent in the track data. As the difference was not very marked,

TABLE 4

Summary of parameters used in simulating the opposed right-turn case

Parameter	Description
Arrival Pattern	Vehicle headways drawn from negative exponential distribution with mean equal to the inverse of the arrival rate. Minimum headway = 1 s (light vehicles).
Discharge Pattern	*Saturated*—constant headways assumed: Straight ahead light vehicles—2 s Straight ahead heavy vehicles—4 s Right turning light vehicles—2.5 s Right turning heavy vehicles—4 s *Unsaturated*—as arrival pattern above.
Gap-Acceptance	Gap-acceptance requirement of leading right turner drawn from lognormal distribution. For single lane opposing flow, average gap required = 4.75 s (variance = 1.84). For dual lane opposing flow, average gap required = 5.26 s (variance = 2.25). Minimum gap accepted = 1.6 s Maximum gap accepted = 9.1 s
Move-up time	Constant value of 2.5 s taken for light and heavy vehicles. For an unopposed movement, this would correspond to a radius (r) of 6 m, and represents the effects of compound curves in the vehicle paths (see Kimber and Semmens 1982).
Storage Space	The space Ns (in numbers of vehicles) available inside the intersection for right turners to queue, varied from 0 to 3.
Proportion of right turners in ahead/right lane	ranged from 0 to 1.
Percentage of commercial vehicles	ranged from 0 to 20 per cent
The number of opposing lanes	either 1 or 2
Signal timings	Cycle times varied from 40 to 150 s Green times varied from 15 to 100 s

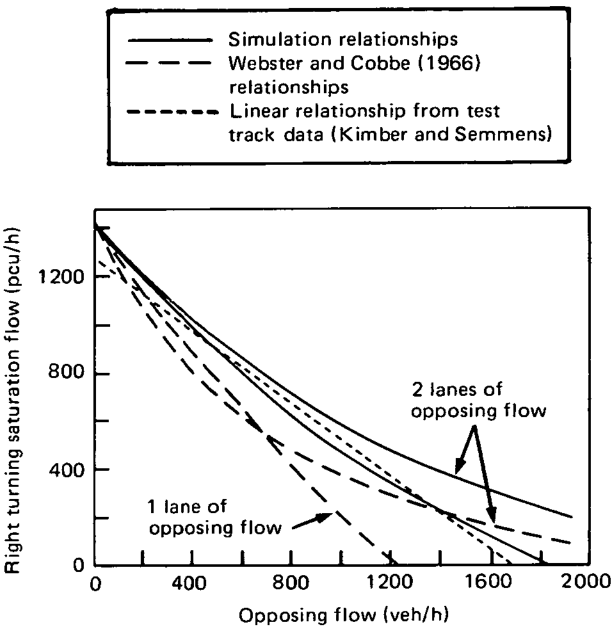

App. B Fig. B1 Relationships between right turning saturation flow and opposing flow for a number of studies

and in view of the difficulty in identifying precise relationships in public road data (eg see Martin and Voorhees Associates (1981)), further refinement of the model was considered unnecessary.

It should be noted, however, that the present results follow from the *assumption* that gap-acceptance completely describes the interaction; the public road data are too variable to enable that assumption to be tested. For give-way junctions—major/minor junctions and roundabouts—other vehicle-vehicle interactions take place (gap-forcing, and gap modification, for example) and significantly modify the capacity. The same may to some extent be true for the opposed right-turn case, although probably less so, but for simplicity we have kept to a simple gap-acceptance description.

Subsequent runs were used to investigate the case $1 \geqslant f \geqslant 0$. Figure B2 shows the form of the results. Inevitably there is an interaction between the effects of q_o and f (since, if f = 1 the dependence of S on q_o must be like that in Figure B1, whereas if f = 0, S is independent of q_o). The curves are also strongly dependent on whether the opposing flow occupies

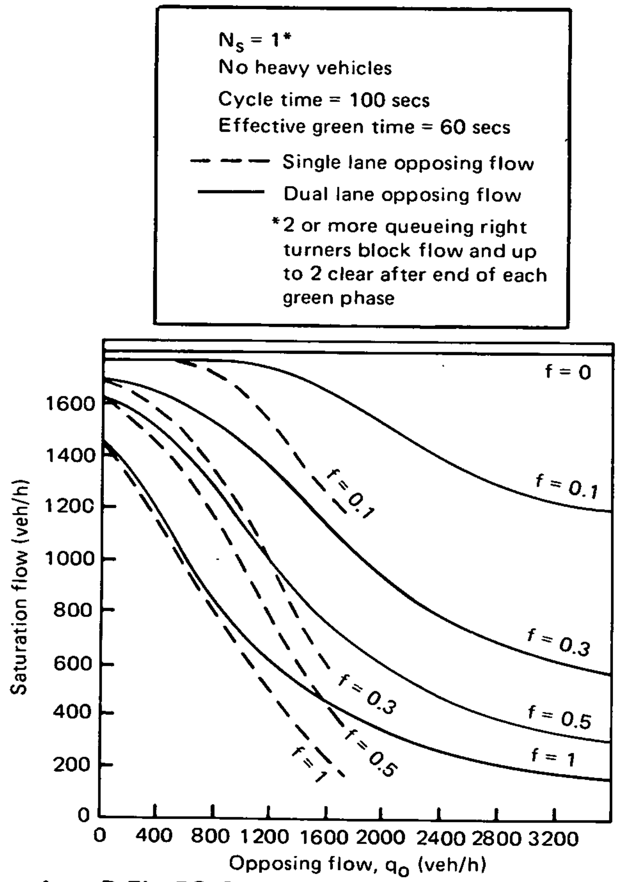

App. B Fig. B2 Saturation flow in ahead/right lane against opposing flow for various proportions of right turners (f)

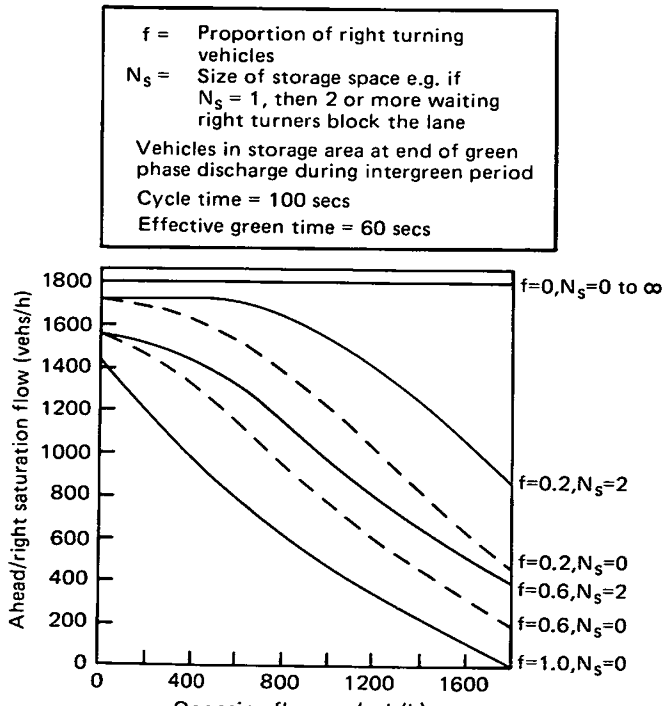

App. B Fig. B3 Saturation flow in an ahead/right lane against opposing flow for various sizes of storage space and according to the simulation

one or two lanes; this results from the minimum headway assumptions for the opposing flow. Figure B3 shows an example of the effects of changes in the storage space.

In principle, simulated data of the type summarised in Figures B2 and B3 could be used simply to build up tables of numerical values which, if calibrated against public road data could be used subsequently for design and assessment purposes. However, it is possible instead to develop a descriptive model which is much more concise and which provides a good representation of the simulation results. Such a model can be constructed from two components: the contribution to the saturation flow from vehicles which depart during the effective green period (S_g) and that from those departing from the storage space immediately following the end of it (S_c).

B.2 A PREDICTIVE MODEL

B.2.1 Departures during the Effective Green

A characteristic of the simulated data is that the dependence of the saturation flow S_g on q_o, n_ℓ, f, r and N_s (n_ℓ is the number of lanes of opposing flow and N_s is the number of storage spaces inside the intersection which right-turners can use without blocking following straight-ahead vehicles) is almost the same when q_o and n_ℓ both change by the same factor; in the main simulated data, n_ℓ took values of 1 or 2 and

$$S_g(q_o, 1, f, r, N_s) \simeq S_g(2q_o, 2, f, r, N_s) \qquad \ldots (A1)$$

So to a good approximation S_g depends only on the ratio (q_o/n_ℓ), f, r, and N_s. (In the simulation r was held effectively constant by employing a constant value of the move-up time for right-turners across all cases considered.) This property can be represented by replacing q_o by the degree of saturation $X_o = q_o/\lambda n_\ell s_o$ where q_o is the opposing flow, c and g are the cycle time and effective green times respectively, and s_o is the saturation flow per lane in the opposing flow, calculated from equation 9. Thus $S_g(q_o, n_\ell, f, r, N_s)$ is replaced by $S_g(X_o, f, r, N_s)$.

This function then has to satisfy certain limiting conditions. Firstly, when the opposing flow is zero it should revert to the form of equation (3) for unopposed flows. The absolute value, A say, of the saturation flow at infinite radius, r→∞, or when there is no turning traffic, f→0 may, however, be different from S_a because of behavioural differences between drivers going straight ahead from mixed lanes containing respectively unopposed and opposed right-turners (because of the possibility of being impeded). Thus the first condition is

$$S_g(0, f, r, N_s) = A/(1 + 1.5\ f/r) \qquad \ldots (A2)$$

Secondly, when all vehicles are right-turners, f = 1, the saturation flow should be independent of the storage space N_s:

$$S_g(X_o, 1, r, N_s) = S_g(X_o, 1, r) \qquad \ldots (A3)$$

Thirdly, when no vehicles are right-turners, S_g should equal the constant A:

$S_g(X_o, 0, r, N_s) = A$ ...(A4)

Finally, when $X_o = 1$, ie the opposing stream is fully saturated (strictly, when $X_o \gg 1$, but for convenience include this with $X_o = 1$), the saturation flow will become zero if $f = 1$, ie all vehicles are right-turners. So

$S_g(1, 1, r, N_s) = 0$ ...(A5)

In the simulation A was set arbitrarily at 1800 pcu/h. A simple form of relation satisfying the constraints (A2)–(A4) can be written

$S_g(X_o, f, r, N_s) = A/(1 + (T-1)f)$ ...(A6)

where: T is the tcu equivalent value of a right-turner as before, but it now depends on X_o, r, f, and N_s: $T = T(X_o, r, f, N_s)$. The constraints (A2)–(A4) together with (A6) suggest the form

$$T(X_o, r, f, N_s) = 1 + \frac{1.5}{r} + t(X_o, f, N_s) \quad \text{...(A7)}$$

where:

(a) because of (A2) and (A6):

$t(0, f, N_s) = 1$ ...(A8)

(b) because of (A3) and (A6)

$t(X_o, 1, N_s) = t_1(X_o, 1)$ ...(A9)

and

(c) because of (A5) and (A6)

$t(1, 1, N_s) = \infty$ ...(A10)

The form required for $t(X_o, f, N_s)$ was investigated by first calculating T^s from

$$\frac{A}{1 + f(T^s - 1)} = S_g^s \quad \text{...(A11)}$$

where S_g^s is the saturation flow obtained from the simulation, over a range of values of X_o, r, f, and N_s. t^s was then calculated from

$t^s = T^s - (1 + 1.5/r)$

(with $(1.5/r) = 0.25$). An example of a plot of t^s against X_o (keeping f and N_s constant) is shown in Figure B4. t^s depends somewhat on the phase length also, and the set of simulated cases included phases of durations from about 30–60 seconds. The dependence on phase length was not strong, however, and was not therefore represented explicitly in the equations. The simplest form of t (X_o, f, N_s) describing the data satisfactorily and satisfying the constraints (A8)–(A10) was

$t(X_o, f, N_s) = [t_1(X_o, f)]/t_2(f, N_s)$ ...(A12)

$$\text{where } t_1(X_o, f) = \frac{aX_o^n}{1 - (fX_o)^m} \quad \text{...(A13)}$$

and $t_2(f, N_s) = 1 + b(1-f)N_s$ ...(A14)

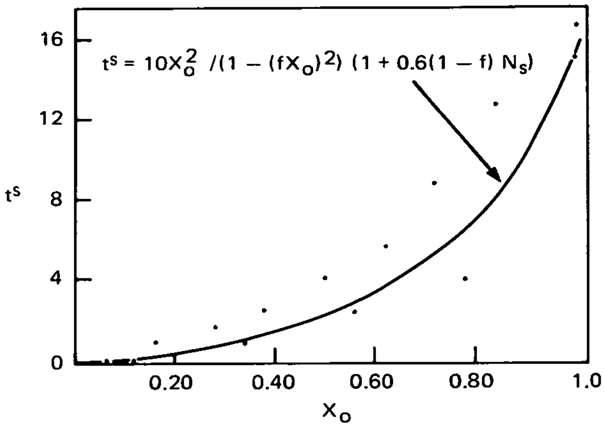

App.B Fig. B4 Relationship between t^s and X_o for $f = 0.7$ and $N_s = 2$
(symbols defined in Appendix A)

where a, b, n, and m are parameters to be determined. The best fit to the data was determined using hill-climbing techniques designed to minimise the sum of squares of the residuals ($S_g^s - S_g^p$) (where S_g^p is as predicted from equations (A6), (A7), and (A12)–(A14)). The result was $a = 10$, $n = m = 2$, $b = 0.6$. Non-integer values for a, n, m did not significantly improve the fit.

To summarise, the final model for S_g was therefore:

$$\left.\begin{aligned} S_g &= A/(1 + (T-1)f) \quad \text{pcu/h} \\ \text{where } T &= 1 + 1.5/r + t_1/t_2 \\ t_1 &= 10X_o^2/(1 - (fX_o)^2) \\ t_2 &= 1 + 0.6(1-f)N_s \end{aligned}\right\} \quad \text{...(A15)}$$

Over the cases simulated, the rms error of this model was 142 pcu/h.

B.2.2 Departures after the Effective Green

At the end of each effective green period right-turners still waiting within the junction depart. The average number departing in a cycle can be written as the product of the total space available for waiting right-turners and an occupancy figure, F, representing the average proportion (over many cycles) of that space occupied at the end of the green phase. Since N_s represents the storage space available (in vehicles) before straight-ahead vehicles are blocked, the total available waiting space for right-turners is $(N_s + 1)$, because when $N_s = 0$, one right-turner can wait. The number departing per cycle is therefore $(N_s + 1)F$.

Values of F obtained from the simulation were found to depend on f and X_o, and increased from zero when $f = 0$ or $X_o = 0$, or both, to unity when $f = X_o = 1$. The best simple form of $F(f, X_o)$ was the function:

$F(f, X_o) = f^m X_o^q$ ...(A16)

Best fit values of m and q were determined by regressing ℓnF_s on ℓnf and ℓnX_o where F_s is the value of F obtained from the simulation. The result was $m = 0.18$ and $q = 0.20$, but the predictive accuracy of the function was not significantly impaired by the constraint $m = q$, and the simple function shown in equation (A17) worked well overall.

$$F(f, X_o) = (fX_o)^{0.2} \qquad \ldots (A17)$$

The rms error $\left\{ (\Sigma (F_s - F_p)^2)/(N-1) \right\}^{\frac{1}{2}}$ was about 0.2.

For the purpose of saturation flow calculations, it is most convenient to include vehicles departing after the end of the green in this way with those departing during the green. Treated in this way, they contribute an amount S_c to the total saturation flow, where

$$S_c = (1 + N_s)(fX_o)^{0.2} . 3600/\lambda c \qquad \ldots (A18)$$

which is in vehicles per hour of effective green. S_c can be written in pcu per hour of effective green by multiplying by a factor P:

$$P = 1 + \sum_i (\alpha_i - 1)p_i \qquad \ldots (A19)$$

where p_i is the proportion of vehicle type i in the traffic and α_i the corresponding pcu value. Thus:

$$S_c = P . (1 + N_s)(fX_o)^{0.2} . 3600/\lambda c \quad \text{pcu/h} \qquad \ldots (A20).$$

Printed in the UK for HMSO by Hobbs the Printers of Southampton
(2253) Dd8222677 9/86 G426